STUDIA INFORMATICA 2009
Volume 30 Number 4 (87)

Andrzej ZACHER
Politechnika Śląska, Instytut Informatyki

INITIAL ANGLE OF LIGHT RAYS AND THEIR INFLUENCE ON THE TOTAL DISTRIBUTION, SCATTERING AND ABSORPTION IN HUMAN TISSUE[1]

Summary. This paper describes the method of light transport in human colon tissue. The structure is treated as a turbid medium, so that subsurface scattering model can be applied. Extended photon mapping algorithm is utilized to add a contribution of fluorescence phenomenon and finally generate images. The quantitative dependencies between photon's angle of incidence and their distribution in the tissue are going to be shown. This investigation can be later used to find the best position of endoscope during cancer seeking and recognition.

Keywords: photodynamic diagnosis, light transport simulation, subsurface scattering, fluorescence model, photon mapping, endoscopy

WPŁYW KĄTA PADANIA PROMIENI ŚWIATŁA NA ICH ROZPROSZENIE, ABSORBCJE I ROZKŁAD W TKANCE LUDZKIEJ

Streszczenie. Artykuł opisuje metodę transportu światła w tkance ludzkiej jelita grubego. Tkanka jest traktowana jako struktura pylasta, dlatego można było zastosować dla niej model podpowierzchniowego rozpraszania. Użyto rozszerzonego o zjawisko fluorescencji algorytmu mapowania fotonów, aby wygenerować obrazy. Pokazano ilościowo wpływ kąta padania fotonów światła na ich rozkład w tkance. Badania te będą mogły zostać użyte w celu znalezienia najlepszego ułożenia głowicy endoskopu i szybszego wykrycia raka.

Słowa kluczowe: diagnoza fotodynamiczna, symulacja transportu światła, rozpraszanie podpowierzchniowe, model fluorescencji, mapowanie fotonów, endoskopia

[1] Supported by Ministry of Science and Higher Education grant R13 046 02

1. Introduction

The Photon Map algorithm was developed in 1993-1994. First papers about this method were published in 1995. This is a comprehensive algorithm that is able to simulate most of global illuminations effects like diffuse inter-reflections, caustic and participating media in complex scenes. It has the same flexibility as normal Monte Carlo ray tracing method, but computational time is reduced.

The global illumination algorithm that benefits from Photon Maps is a two-pass method. The first pass builds the photon map by emitting photons from the light sources into the scene and put them in the special structure called Photon Map when they hit non-specular objects. In the second pass rendering is done. It uses statistical techniques to extract information about incoming flux and reflected radiance from Photon Map for any point in the scene.

Compared to other method of global illumination Photon Maps have many advantages. It is relatively fast even for complex scenes and handles non-diffuse surfaces and caustic effects. Low frequency noise, efficiency, quality of final images and reasonable memory usage for storing the photons, make this algorithm one of the most important in computer graphics. Normal Monte Carlo ray tracing methods such as path tracing, bidirectional path tracing and Metropolis are out of date [1].

In order to describe the model of light transport in human tissue, some additional computations need to be performed besides normal Photon Mapping. Reflection of a photon at air-tissue or tissue-tissue boundaries must be calculated. Once entered the tissue, the photon is moved a given distance where it may be absorbed, scattered, reflected internally or out of the tissue. To generate new scattering angles inside the object, phase function may be utilized. The photon is repetitively moved until it either is completely absorbed or escapes from the tissue. If the photon is absorbed, the position of that incident is recorded. If the photon escapes from the tissue, the transmission or reflection of the photon is stored. This procedure is repeated until the desired number of photons have been traced and recorded. As the number of photons propagated approaches infinity, the overall reflection, transmission, and absorption profiles approach real values. This data can be later compared with medical investigations for the tissue with similar optical properties [2].

The distribution of the photons on the surface of the tissue, their properties like energy, spectrum and escape angle are going to be analyzed. This values are different for various adjustments of the light source, especially its angle of incidence. The maximal depth, the photon penetrated the tissue, will be investigated as well.

It is not the purpose of this paper to concentrate on the structure and fluorescent properties of a human tissue. This model was introduced in [3] and in this paper it is going to

be only shortly described. More details about fluorescence from endogenous and exogenous molecules in cells and tissues, especially in vivo and ex vivo studies can be found here [4].

2. Previous work

[3] presents Monte Carlo model of steady-state light transport in multi-layered tissue and describes local rules of photon propagation. When a scattering event occurs, the angle of deflection in a photon trajectory and the step size of photon movement during photon-tissue interaction depend on probability distribution functions. The simple model of tissue with parameters was introduced as well, but without fluorescent properties. Such features as phase and polarization of the light are ignored. Because of the fact that the method is statistical in nature and relies on calculating the propagation of a large number of photon, it requires a large amount of computation time. Despite of all those restrictions, it can be still used and applied to simulate light transport correctly.

Subsurface light transport in translucent materials was presented in [5]. It extends common BRDF model to capture such effects as color bleeding within materials and diffusion of light across shadow boundaries, where the light that entered a material leaves it at different position (BSSRDF). The main idea utilizes an exact solution for single scattering with a dipole point source diffusion approximation for multiple scattering. However, it is not straightforward to simulate fluorescent properties of tissues using this model.

In this paper [6], Monte Carlo predictions and diffusion models for homogeneous media are compared with properties characteristic of highly light-scattering tissues. There was discussed the relative advantages and disadvantages of the two models and computations of radiance, fluence and reflectance were presented. Also, some graphs and sketches were presented showing radiance in different directions (relative to the incident infinite beam) versus depth, depending on optical properties, influence of albedo and relative index of refraction. Additionally polar plots of radiance at different depths for a scattering medium were introduced.

In [7] model for subsurface scattering in layered surfaces in terms of one-dimensional linear transport theory was presented. The external appearance of a face and a cluster of leaves from experimental data describing their layer properties, were simulated. It also showed how volume or surface functions (BRDF and BTDF) change for different values of anisotropy and thickness of the layer. Finally, it was described how various angles of incidence influence surface and subsurface components of the reflection model.

Global illumination in scenes with participating media was introduced in [8]. The algorithm is focused on bidirectional Monte Carlo ray tracing and uses photon maps to

reduce noise and increase efficiency. The idea of photon map was extended. Besides surface, also volume photon map containing photons in participating media was used. It was also needed to derive a new radiance estimate for photons in the volume photon map. This method could effectively simulate effects such as multiple volume scattering, color bleeding between volumes and surfaces, and volume caustics.

This paper does not concentrate on creating human tissue model. It utilizes one layer model that is a simplification of the multilayer structure presented here [9]. Fluorescent properties of a tissue and contribution of different substances to final spectrum intensity was described in [10].

Although the light propagation in human tissue is rather good known topic described in literature, the quantitative analysis of its properties and influence of incident angle on absorption and scattering of photons need to be still investigated. Simulations in this is paper are going to propose the best initial angle of light source, for witch energy reflected from the tissue to camera is the highest.

3. Human tissue properties

Snow, plants, milk, human skin, marble etc. are frequently encountered in the natural world. There are perceived as translucent, because their appearance is distinctly smooth and soft as a result of light scattering inside the objects. The scattered light gets diffused and blurs the effect of small geometric details on the surface, softening the overall look. Moreover, scattered light can pass through translucent structures. This effect is especially noticeable when the structure is lit from behind. To capture the true appearance of translucent materials and render these phenomena, it is therefore necessary to simulate subsurface scattering, where the light leaves the object at different position than it was initially captured [11].

In [3] the following model was described, which was proved by laboratory investigations. The human tissue was infinitely long and wide single-layered structure with thickness long enough to absorb all the light. It was characterized by refractive index n_{layer}=1.1, absorption coefficient u_a=20cm^{-1} (the probability of photon being absorbed per unit infinitesimal pathlength), scattering coefficient u_s=200cm^{-1} (the probability of photon being scattered per unit infinitesimal pathlength) and the anisotropy factor g=0.9 (the average of cosine value of deflection angle). The top ambient medium was air with refractive index equal to 1.

However the light is not only absorbed and scattered under the surface of the object, but also its spectrum changes relatively to material the tissue consists of. To model the influence of fluorescence phenomenon, collagen and photofrin molecules were chosen as dominant fluorophores. The probability of interaction a photon sample with a fluorophores was defined

as $d_{collagen}$=0.2 and $d_{photofrin}$=0.1. Moreover, the concentration of fluorescent molecules in fluorophore is different for each substance and described as $c_{collagen}$=0.4 and $c_{photofrin}$=0.33. All these values can be easily parameterized.

The last factor that characterizes each fluorophore is Excitation-emission matrix (EEM). It uniquely describes the emission spectra as a function of excitation spectrum [12]. The fluorescence EEMs of mentioned fluorophores was measured using standard fluorescence spectrophotometer [13].

4. Light transport and two types of photon map

A photon map is a data structure, usually a balanced kd-tree, created to store information about photon hits. Each node of the kd-tree contains the data about the coordinates of the hit point (x, y, z), color spectrum, incident direction of the photon, and other important information. Depending on the place where the photon undergoes the interaction with tissue, surface and volumetric photon map were created; Surface photon map for photons located only on the surface of the tissue, volumetric photon map for photons inside.

Photon mapping belongs to the group of particle tracing algorithms, which are based on the idea of creating paths from the light sources. It tries to separate the representation of a scene from its geometry and collects illumination information in a data structure, the surface photon map [14]. Each photon packet was assigned a spectrum with energy proportional to the spectrum of the light source. That radiance of a photon, described by its color spectrum, expresses its weight W.

Photon mapping is a two-pass method. In the first step, photons are generated and shot into the scene using Halton sequence. When a photon hits an object, utilizing Snell's law, incident reflectance $R(a_i)$ is calculated and compared with random number. It determines whether the packet is reflected back or enters the tissue. Since the photon interacted with tissue, its weight needs to be decreased:

$$W = W - WR(a_i) \tag{1}$$

Then the position of the packet is changed in the initial direction by the step size defined as:

$$s = -\frac{\ln(\xi)}{u_a + u_s} \tag{2}$$

where ξ is a random number. Once the photon was moved, some attenuation of the photon weight must be computed, due to absorption by the interaction site.

$$W = W - W\frac{u_a}{u_a + u_s} \tag{3}$$

Now is the time to determine if the interaction happened with one of fluorophores or with other substance the human tissue consists of. Another two random numbers are generated and compared with the probability of interaction a photon with fluorophore *d* and then the concentration of fluorescent molecules in fluorphore *c*. If the fluorescent phenomenon occurred the spectrum of the photon is updated according to EEM. Moreover, the photon's spectrum, position and its direction is stored in volumetric photon map. From now on this photon is marked as fluorescent and its properties are going to be stored in the photon map after every movement inside tissue, until it is completely absorbed. Data from the volumetric photon map will be used to generate images only.

Finally, once the weight and spectrum of the photon was updated, the packet is ready to be scattered. The cosine of deflection angle can be calculated from Heney-Greenstein phase function as a scattering function of random variable and albedo *g*. Additionally, the azimuthal angle is proportional to an additional random variable multiplied by 2π. This process of moving, absorbing and scattering a packet is repeated until either the weight of the photon is too small or the photon hits the tissue interface again and escapes. If this is a case and if the photon is fluorescent, then it is stored in the surface photon map. Data especially from this kind of structure is going to be analyzed carefully in this paper. It is also necessary to add, that in every loop a Russian Roulette is performed to check whether photon sample should be terminated or should survive [3].

In the second pass of the algorithm the scene is rendered with the help of the photon maps built in the first pass. An usual ray tracing process is performed by shooting rays from the camera. When a ray hits a given point on a surface, the illumination information of the neighboring photons is collected and added to the radiance information collected from ray tracing at that point [11].

It was assumed that the tissue surface is not Lambertian surface, which means that the illumination at the point in all directions is not the same. A little specular appearance was added to the tissue, so that the radiance is angle dependent and can be modified by simple Gauss function.

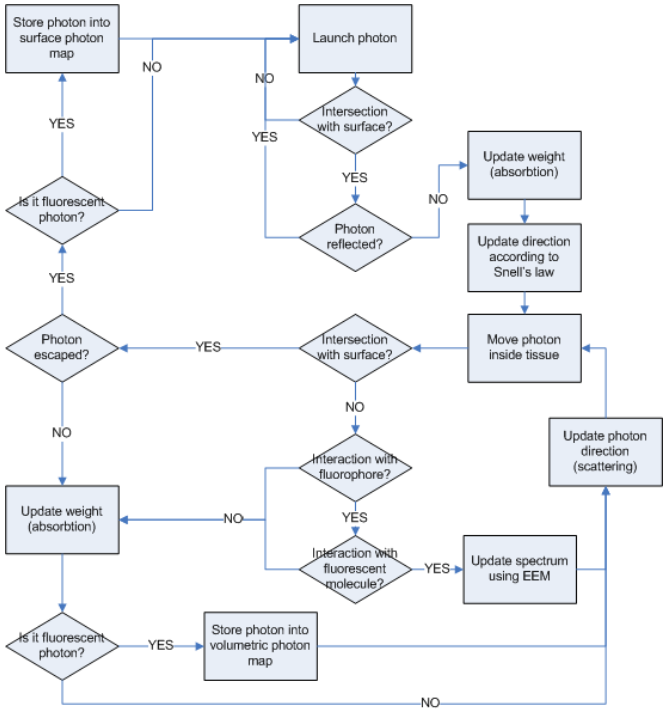

Fig. 1. Flow diagram of proposed Monte Carlo model
Rys. 1. Diagram przejść zaproponowanego modelu Monte Carlo

5. Simulation and results

The simulation was performed for infinitely thick single-layered tissue. Moreover cancerous polyp was added into the tissue model in which, besides collagen, also photofrin was concentrated.

The light sources and camera imitate the real endoscope and are presented in details below.

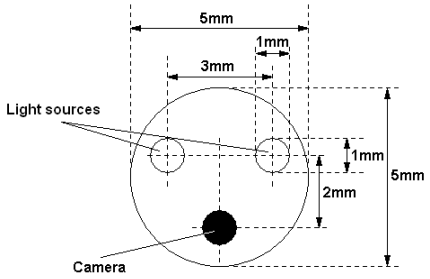

Fig. 2. The head of endoscope – bottom-view. Device parameters are close to the real
Rys. 2. Głowica endoskopu – widok od dołu. Parametry urządzenia są zbliżone do rzeczywistych

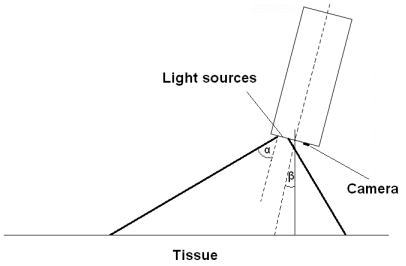

Fig. 3. The head of endoscope – side-view
Rys. 3. Głowica endoskopu – widok z boku

Both light sources are assumed to be white area lights with cone angle α=15°. Additionally the head of endoscope may be rotated. Angle β specifies the deviation from the

perpendicular position with respect to tissue surface. The influence of changing this angle is going to be investigated.

The graphic engine that was used to simulate photon mapping and generating images was PBRT. This computer program was written completely in C++ and was initially designed for university purposes. The source code of PBRT is available with the book [15] that gives highly detailed description of most of the functions. Speed and efficiency are not the advantages of this software. To render highly detailed and complex images it takes often minutes or even hours. Unfortunately subsurface scattering model is not supported by PBRT. The photon mapping algorithm needed to be rewritten to realize full Monte Carlo model of Light Transport in turbid media.

In the described scene 12 simulations were performed, each for different angle β. In each case 500000 photons were stored in surface photon map. Photons collected in volumetric photon map were neglected this time. The investigation started for β=0° and was changed by 5° every time.

In order to store half of million fluorescent photons in surface photon map, it was necessary to trace more than one million photon in the scene. It means that 50% of them was absorbed by the tissue and after entering the structure, they never escaped. Fig. 4 describes how many photons were needed to store exactly 0.5 million of photons on the surface.

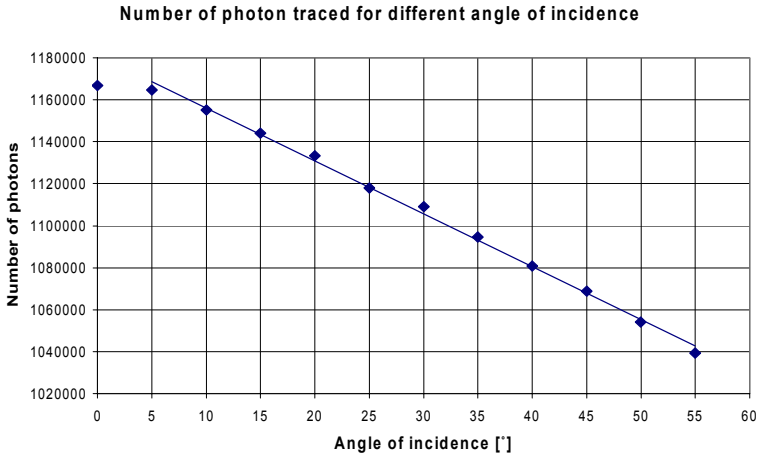

Fig. 4. Number of photons vs. angle of incidence
Rys. 4. Zależność między liczbą fotonów a kątem padania

For angles around β=0°, where the endoscope is completely perpendicular to the tissue surface, the number of photons taking part in the simulation is more or less constant. When the angle exceeds 5°, perfectly linear behavior is observed. The graph is going down, which means that less number of photons is needed when the angle of view gets increased. For small angles the tissue absorbs energy of the light rays to the grater extent than for angels around β=50°. The difference of number of photons needed in boundary cases, tends to even 11%.

Next, energy of photons were investigated. Each photon traced from the light source has the same, constant energy. That energy changes during contact with tissue, the photon can be absorbed, scattered or its spectrum (energy) may be altered. In the end of simulation, the energy of each photon stored in the surface photon map was summed up, giving the total power. The following graph represents the normalized overall energy of photons for different angle of camera.

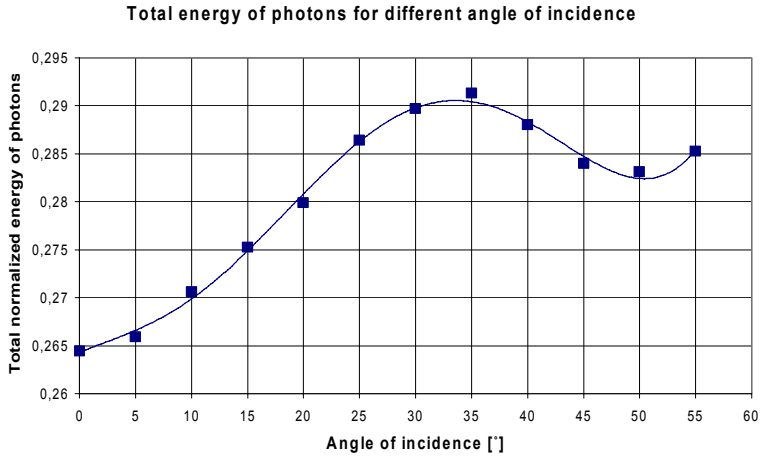

Fig. 5. Total energy of photons vs. angle of incidence
Rys. 5. Zależność między całkowitą energią fotonów a kątem padania

The investigation shows that the lowest energy was observed for angle β=0°. It means that in such a situation packets of energy get involved into different interactions inside tissue more often than for other angles. They lose their power many times before they finally gets back to the tissue surface and escapes. It proves again that for small angles the absorption is a dominant factor.

The situation changes when the angle of incidence is increased. Two local extremes are observed on the plot. Local minimum is not interesting for further investigations, the goal is to find the angle for which the total energy of all photons is the greatest. This is why the polynomial of sixth degree was applied to the data, giving the local maximum of the graph. For incident angle around 34°, the energy stored on the tissue surface is the highest. Probably angles around this value should be investigated more deeply during other experiments. At this moment, it gives medicine the first hint about the most accurate angle of the head of endoscope in relation to tissue surface, for which pathological changes inside the structure are the best visible.

Another experiment was concentrated on the directions of all photons stored on the surface photon map. For each packet it was checked if it is visible on the camera screen. If it is true, then the angle between photon exitant vector and vector pointing from the packet to camera position was calculated. If that angle was not greater than 15°, that photon was assumed to play essential role in the image rendering process and marked as important. Their

influence should be more noticeable, than contribution of photons pointing in other directions. The more packets that are "important" were stored in photon map, the better quality of the final image is going to be.

Fig. 6 shows how the number of photons, we are interested in, changes for different angles the endoscope is working.

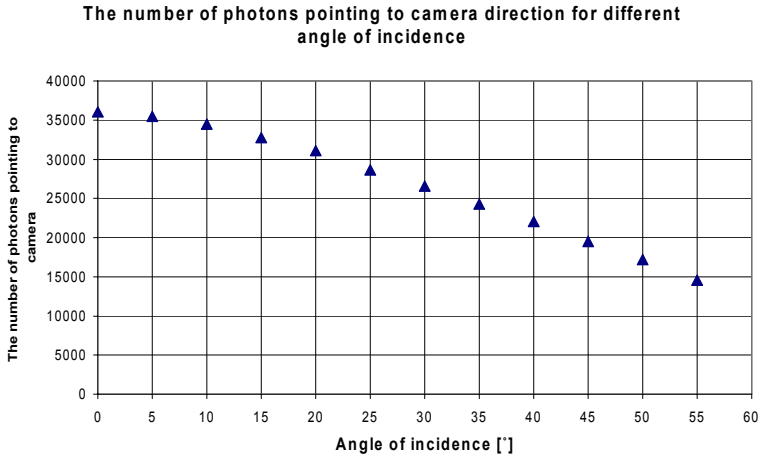

Fig. 6. The number of photons pointing to camera vs. angle of incidence.
Rys. 6. Zależność między liczbą fotonów skierowanych w kierunku kamery a kątem padania

The plot above can be treated as linear again. It is interesting that in the best case not even 10% of all the photons stored in the map, fulfill our criterion. For angle $\beta=55°$ it is only about 3%. The function is decreasing, so the best looking images should be obtained for endoscope perpendicular position. But it is not necessarily true, because the investigation didn't take into account the energy of the photons. Probably some of them have proper exitant direction, but its energy is so small that they can be neglected. This simulation needs additional power related criterion in order to draw more accurate conclusions.

In the one but last simulation some work has been done to investigate what was the maximum depth the photon is able to go through. For each photon the deepest value was taken, but only the highest from all of them was drawn on the plot.

Fig. 7. describes how the maximal depth of penetration changes for different angle of view. Basically it does not change when increasing angle of incidence and remains at the constant level of -0.12 cm. In particular cases the values are greater or smaller from the mean depth, but no correlation could be observed with the initial angle. This is a simulation error, which would be smaller if the greater number of photons were traced. In such a case packets would be distributed in the tissue more evenly and not only one – as it is now – but many photons, would indicate the maximal depth the photon is able to enter.

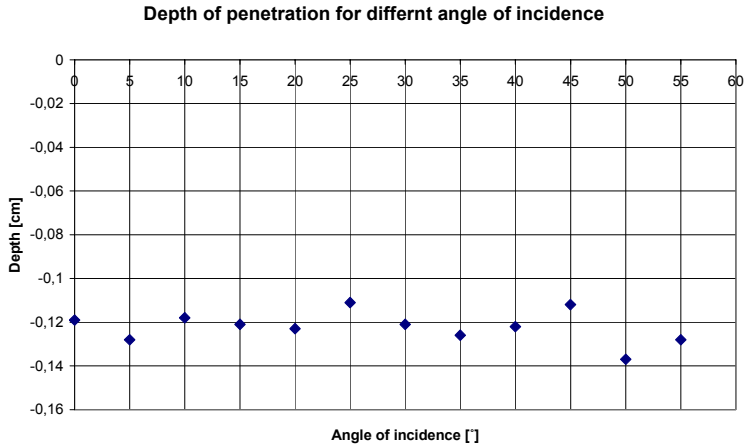

Fig. 7. Depth of penetration vs. angle of incidence
Rys. 7. Zależność między głębokością penetracji a kątem padania

Finally, each photon excitant vector was placed in the center of hemisphere. The hemisphere was divided into 3D bins: vertically into 10 bins – each equal to 9°, horizontally into 36 bins – each equal to 10°.

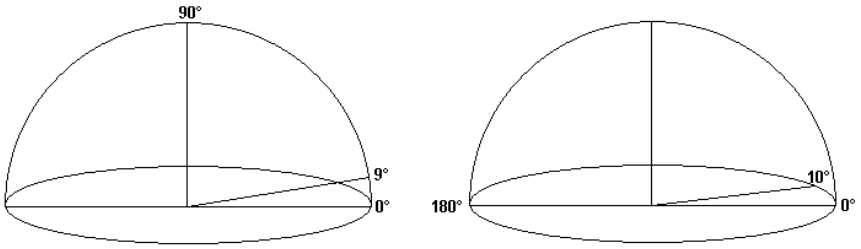

Fig. 8. Division of the hemisphere into bins 9° wide vertically and 10° wide horizontally. Together 360 bins
Rys. 8. Podział hemisfery na części: 9° wertykalnie i 10° horyzontalnie. Łącznie 360 części

Each photon was then placed into one and only one bin in the hemisphere, appropriate for the exitant direction. The number of packets in every bin was counted and drawn in the polar coordinate system. First column represents vertical angles in range between 45÷90°, the second is for range between 0÷45°.

Figure 9 show the distribution of excitant directions of photons in the tissue for different angle of incidence β.

For β=0° (Fig. 9a) each polar plot representing one vertical direction looks like a circle, what means that for light perpendicular direction, exitant vectors of all the photons are equally distributed. It proves that light propagation algorithm is not biased in any way.

When the angle of incidence grows, small changes in the shape of each circle are observed. They gets ellipsoidal in shape and shifted along vector pointing 180°. However, those changes start for small vertical angles and after that other levels are affected. It means that distribution of angles above 45° remains almost unchanged for different light views. Their shape on the polar plot is only little ellipsoidal and the amplitude gets smaller.

For the angle of incidence equal to 50° there are 2 bins containing more than 10000 photons pointing along horizontal 180° direction. These are photons with vertical angle not greater than 10°. Then other ellipsoidal plots are visible with gradually smaller distortions in shape.

It is needed to stress out, that the effect described above is observable for small view angles of light α only. The narrower the light beam is, the more noticeable this effect appears.

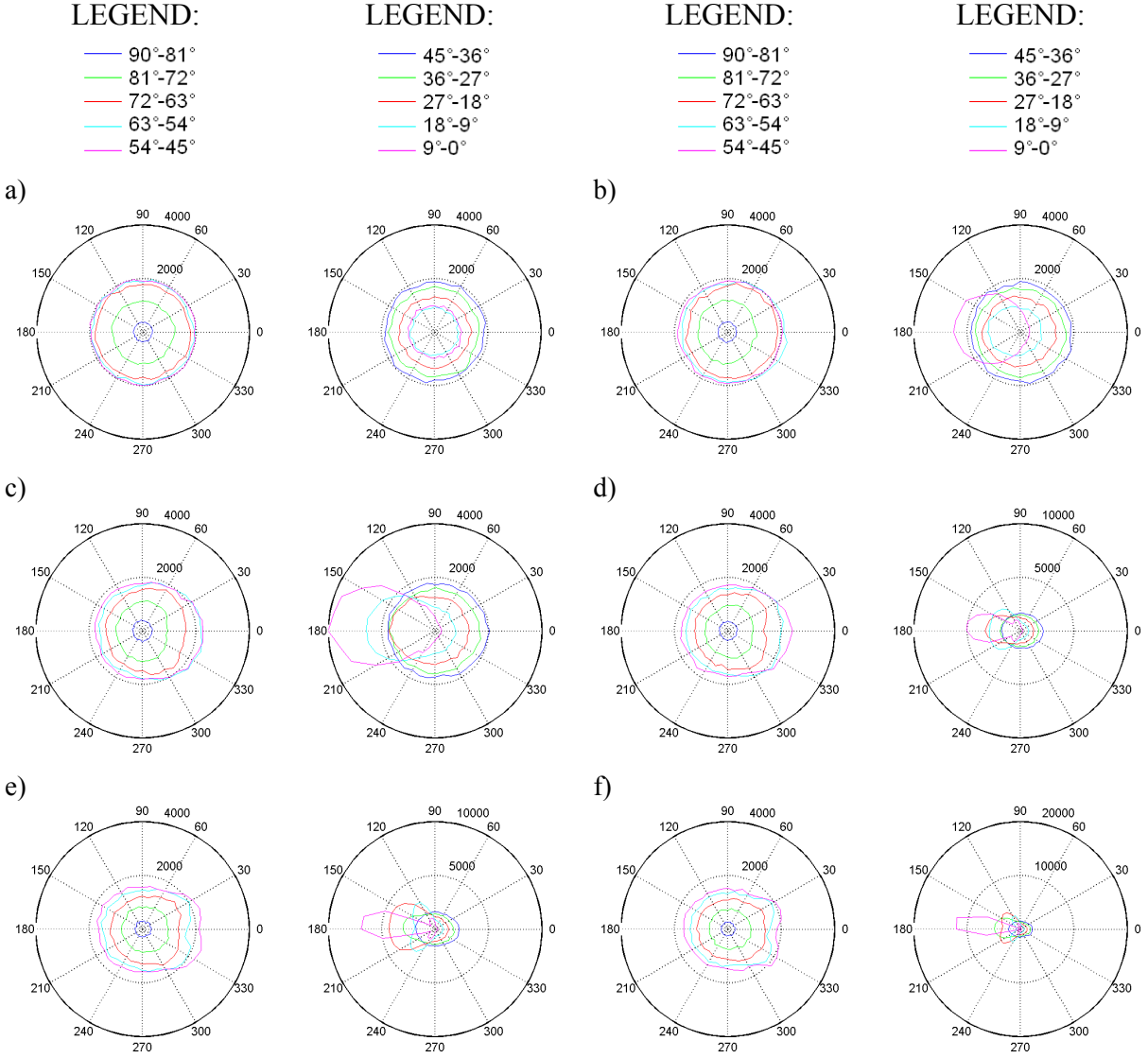

Fig. 9. Distribution of photon exitant directions for: a) β=0, b) β=10, c) β=20, d) β=30, e) β=40, f) β=50
Rys. 9. Rozkład wektorów wyjścia fotonów dla: β=0, b) β=10, c) β=20, d) β=30, e) β=40, f) β=50

6. Discussion and future work

All of these experiments prove, that the tissue model and chosen algorithm of light transport in turbid media are mathematically correct and give expected results. Increasing the

initial angle of incidence, less photons get absorbed and more of them escapes the tissue. The shape of graph representing total energy of photons vs. angle β, shows that this relation is not linear and some local maximums and minimums can be found. This surprising result give some hints about the best incident angle, for which changes in tissue structure are better observable. By isolating photons, that after exiting the tissue was directed to the camera location, it was noticed that their number also changes in linear way. It is also correct, once camera and light sources are in the same place, escaping photons should not point back in the direction they entered the object. Analyzing the maximal depth the packets penetrated the tissue for different cases, it seems to be constant as it was expected. Further investigations should concentrate on the vertical profile i.e. the distribution of the deepest photons in the structure. This is going to give some idea about, what is going on inside the tissue. Consideration of the exitant vector distribution also gives interesting result. It proved that the number of photons having vertical angle greater than 45° does not change and is constant for different initial angle β. On the other hand, number of packets directed along 180° horizontally increased enormously.

This quantitative analysis describes what is happening with photons contacting with human tissue. It also proposes the range of angles β for which the influence of photons on final image should be the highest. This conclusions should be now compared with generated images and probably verified with real images. This challenging is going to be the subject of the another paper.

BIBLIOGRAPHY

1. Christensen P. H., Jensen H. W., Kato T., Suykens F.: A practical guide to global illumination using photon mapping. Siggraph 2002, Course 43.
2. Prahl S. A., Keijzer M., Jacques S. L., Welch A. J.: A Monte Carlo model of light propagation in tissue. SPIE Proceedings of Dosimetry of Laser Radiation in Medicine and Biology, IS 5, 1989, p. 102÷111.
3. Wang L., Jacques S. L.: Monte Carlo modeling of light transport in multi-layered tissues in standard C. University of Texas M. D. Anderson Cancer Center 1992.
4. Latos W., Kawczyk-Krupka A., Ledwon A., Kosciarz-Grzesiok A., Misiak A., Sieron-Stoltny K., Sieron A.: The role of autofluorescence colonoscopy in diagnosis and management of Solitary Rectal Ulcer Syndrome. SPIE Photonics West- Conferences and Courses. Biomedical Optics. Imaging, Manipulation and analysis of Biomolecules, Cells and Tissues VI. Cell and tissue functional imaging. San Jose 2008.

5. Jensen H. W., Marschner S. R., Levoy M., Hanrahan P.: A practical model for subsurface light transport. In Proceedings to Siggraph, 2001, p. 511÷518.
6. Flock S. T., Patterson M. S., Wilson B. C., Wyman D. R.: Monte Carlo modeling of light propagation in highly scattering tissues-I: Model predictions and comparison with diffusion theory. IEEE Transactions on Biomedical Engineering, Vol. 36, No. 12, December 1989.
7. Hanrahan P., Krueger W.: Reflection from layered surfaces due to subsurface scattering. Computer Graphics (Proc. SIGGRAPH 1993), July 1993.
8. Jensen H. W., Christensen P. H.: Efficient simulation of light transport in scenes with participating media using photon maps. In Proceedings of SIGGRAPH'98, Orlando, July 1998, p. 311÷320.
9. Zeng H., MacAulayl C., McLean D. I., Palcic B., Lui H.: The dynamics of laser-induced changes in human skin autofluorescence – Experimental measurements and theoretical modeling. Photochemistry and Photobiology, 68(2), 1998, p. 227÷236.
10. Drakaki E., Makropoulu M., Serafetinides A. A.: In vitro fluorescence measurements and Monte Carlo simulation of laser irradiation propagation in porcine skin tissue. Lasers in medical science, 23(3), 2008, 267÷276.
11. Jensen H. W., Buhler J.: A rapid hierarchical rendering technique for translucent materials. ACM Transactions on Graphics (SIGGRAPH'2002), Vol. 21, issue 3, San Antonio, July 2002, p. 576÷581.
12. Li BH., Xie SS.: Autofluorescence excitation-emission matrices for diagnosis of colonic cancer. World J Gastroenterol, 11(25), 2005, p. 3931÷3934.
13. Dacosta R. S., Andersson H., Wilson B. C.: Molecular fluorescence excitation–emission matrices relevant to tissue spectroscopy. Photochem Photobiol, 78(4), 2003, p. 384÷392.
14. Yu TT., Lowther J., Shene CK.: Photon mapping made easy. SIGCSE'05, February 23–27, 2005, St. Louis, Missouri, USA.
15. Pharr M., Humphereys G.: Physically based rendering. From theory to implementation. Morgan Kaufmann, 2004.

Recenzent: Dr hab. inż. Maria Pietruszka, prof. Pol. Łódzkiej

Wpłynęło do Redakcji 14 lipca 2009 r.

Omówienie

Materiały spotykane w życiu codziennym, takie jak mleko, płatki śniegu, liście roślin, skóra ludzka mają tę specyficzną właściwość, że promienie światła nie rozpraszają się wyłącznie na ich powierzchni. Wnikają do środka, przemieszczają się pod powierzchnią, są absorbowane, rozpraszane, a w niektórych przypadkach nawet ich widmo ulega zmianie. Część z nich zostaje kompletnie wchłonięta, reszta powraca na powierzchnie, jednak w zupełnie innym miejscu. Badanie rozkładu właśnie tego światła – reprezentowanego przez fotony – w zależności od kąta padania, pozwoli znaleźć jego najbardziej optymalną wartość.

Aby zasymulować opisane wyżej zjawisko w stosunku do tkanki jelita grubego, zdecydowano posłużyć się algorytmem Monte Carlo przedstawionym na rys. 1. Niezbędne w tym celu jest laboratoryjne zidentyfikowanie takich parametrów tkanki, jak współczynniki załamania, absorpcji, rozpraszania światła i anizotropii. Należało także ustalić, z jakich substancji tkanka się składa, w jakiej koncentracji i które z nich posiadają właściwości fluorescencyjne – przyjęto, że kolagen i fotofryna.

Algorytm mapowania fotonów ma zasadniczo dwie fazy. W pierwszej fotony są generowane i wystrzeliwane w kierunku badanego obiektu. Prawo Snella determinuje, czy foton zostaje odbity, czy też wnika pod powierzchnię tkanki. Wtedy jego energia zmniejsza się wg wzoru (1). Następnie foton jest przemieszczany o (2) i ponownie absorbowany (3). Jeśli oprócz tego zajdzie zjawisko fluorescencji, widmo fotonu jest zmieniane na podstawie macierzy EEM. Proces ten trwa tak długo, aż energia fotonu jest zbyt mała, żeby mogła mieć wpływ na oświetlenie tkanki. Jeśli foton ponownie wyjdzie na powierzchnie, jego energia i kąt są mierzone i przedstawiane na wykresach.

Pokazano, że liczba absorbowanych fotonów maleje wraz ze wzrostem kąta padania (rys. 4). Zostało także wykazane, że całkowita energia wszystkich fotonów zależy nieliniowo od kąta początkowego i ma lokalne maksimum przy 34°(rys. 5). Przeanalizowano liczbę fotonów skierowanych w kierunku kamery (rys. 6) i ich liczba jest największa dla kąta 0°, a potem liniowo maleje. Ponadto zbadano maksymalną głębokość, jaką osiągają fotony i jest ona niezależna od kąta padania (rys. 7). Analiza wektorów wyjścia dowiodła, że ilość fotonów skierowanych horyzontalnie wzdłuż kąta 180° bardzo szybko rośnie wraz ze wzrostem nachylenia źródła światła. Rozkład wertykalny natomiast dla kątów powyżej 45° pozostaje mniej więcej stały (rys. 9).

Zgromadzone wyniki mogą sugerować zakres kątów, dla których wygenerowane później obrazy będą najlepiej odwzorowywały zmiany rakowe zachodzące w ludzkich tkankach.

Address

Andrzej ZACHER: Politechnika Śląska, Instytut Informatyki, ul. Akademicka 16,
44-100 Gliwice, Polska, andrzej.zacher@polsl.pl .